Journal of Magnetism and Magnetic Materials 127 (1993) 83–92
North-Holland

Neutron diffraction and magnetic study of the HoNiGe and ErNiGe compounds

G. André [a], F. Bourée [a], A. Bombik [b], A. Olés [b], W. Sikora [b], M. Kolenda [c] and A. Szytuła [c]

[a] *Laboratoire Léon Brillouin (CEA-CNRS), CEN-Saclay, 91191 Gif-Sur-Yvette Cedex, France*
[b] *Department of Physics and Nuclear Techniques, Academy of Mining and Metallurgy, 30-059 Kraków, Poland*
[c] *Institute of Physics, Jagellonian University, 30-059 Kraków, Reymonta 4, Poland*

Received 3 November 1992

HoNiGe and ErNiGe crystallize in an orthorhombic TiNiSi-type structure with the space group Pnma. Neutron diffraction measurements at low temperatures indicate magnetic structures with the wavevectors $k_1 = [1/2, 0, 1/2]$ for HoNiGe and $k_2 = [0, 1/2, 0]$ for ErNiGe. With an increase in temperature, a change in the magnetic structure to a modulated one with the wavevector $k_1' = [0.469, 0.221, 0.426]$ at $T = 2.55$ K for HoNiGe and $k_2' = [0, 0.5, 0.084]$ at $T = 2.36$ K for ErNiGe is observed. The magnetic structures determined are verified by symmetry analysis.

1. Introduction

A large number of ternary rare earth intermetallic compounds with the general formula RTX (where R is a rare earth element, T is a transition 3d element and X is Si or Ge) are known to exist [1–3]. These compounds crystallize in 12 different types of structure [3–5]. Systematic studies of the magnetic properties were performed only for some groups [6]. In this work we present the results of X-ray and neutron diffraction as well as magnetometric measurements undertaken in order to determine the crystal and magnetic structures of HoNiGe and ErNiGe.

The RNiGe compounds crystallize in the orthorhombic TiNiSi-type structure [7]. From magnetometric measurements it follows that the compounds with Gd, Tb, Dy and Er are antiferromagnets the Néel temperatures 11, 7, 9 and 6 K, respectively [7].

Correspondence to: Professor A. Szytuła, Institute of Physics, Jagellonian University, 30-059 Kraków, Reymonta 4, Poland.

2. Experimental details

Both compounds were synthesized by arc melting stoichiometric amounts of the high-purity components. The samples were subsequently annealed in vacuum for 12 days at 800°C. The X-ray diffraction patterns of both compounds consisted of a large number of lines characteristic of an orthorhombic crystal structure. The magnetometric measurements were carried out using a RH–Cahn balance in the temperature range 2–293 K. The neutron diffraction data were obtained by means of the neutron powder diffractometer G4.1 installed at the Orphée reactor (Laboratoire Léon Brillouin, Saclay) with an incident neutron wavelength of 2.426 Å. Neutron scattering lengths were taken from the Delapalme work [8] and the Ho^{3+} and Dy^{3+} form factor was taken from Freeman and Desclaux [9].

Table 1
Crystal structure data for the HoNiGe and ErNiGe compounds

	HoNiGe	ErNiGe
T (K)	30	8
a (Å)	6.852(5)	6.801(3)
b (Å)	4.202(4)	4.188(3)
c (Å)	7.263(8)	7.243(5)
x_R	0	0
z_R	0.7071(4)	0.7048(6)
x_{Ni}	0.1945(2)	0.1935(2)
x_{Ni}	0.0847(3)	0.0983(3)
x_{Ge}	0.3055(2)	0.3065(4)
z_{Ge}	0.4153(3)	0.4017(3)
R (%)	7.84	4.42

3. Results

3.1. Crystal structure

The reflections observed in the neutron diffraction patterns obtained in the paramagnetic region (30 K for HoNiGe and 8 K for ErNiGe compounds) are consistent with the space group Pnma (D_{2h}^{16}) of the orthorhombic TiNiSi structure. The R, Ni and Ge atoms are in 4(c) positions: $x, 1/4, z$; $\bar{x}, 3/4, \bar{z}$; $1/2+x, 1/4, 1/2-z$; $1/2-x, 3/4, 1/2+z$. The experimental data were analyzed by the Rietveld method [10] in which three pairs of (x, y) parameters were subjected to a least-squares calculation. The parameters corresponding to the minimum of the reliability factor are listed in table 1.

3.2. Magnetic properties

The temperature dependence of the magnetic susceptibility of HoNiGe and of ErNiGe have

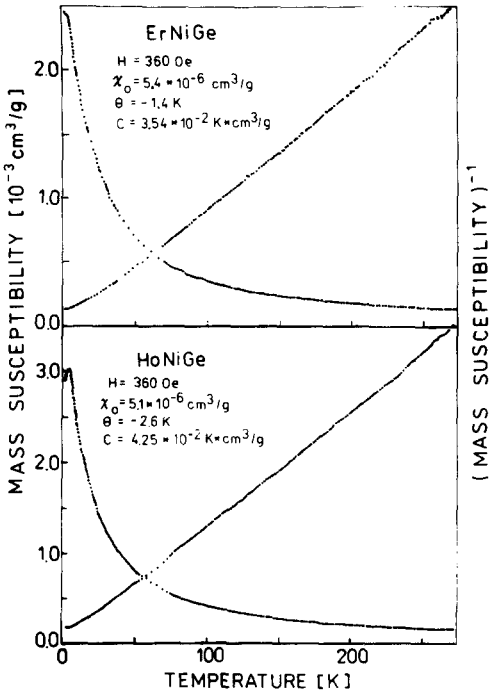

Fig. 1. Temperature dependence of the magnetic susceptibility and reciprocal susceptibility for HoNiGe (a) and ErNiGe (b).

maxima at 5 and 2.9 K, respectively (see fig. 1), which are characteristic of a transition to an antiferromagnetic state. At higher temperatures the magnetic susceptibility is fitted by the relation:

$$\chi = \chi_0 + \frac{C}{T - \Theta_p}.$$

The values of χ_0, effective magnetic moment and paramagnetic Curie temperature are listed in

Table 2
Magnetic data for the HoNiGe and ErNiGe compounds

Compound	T_N (K)	Θ_P (K)	μ_{eff} (μ_B/R^{3+})		χ_0 (cm^3/g)	Ref.
			Exp.	Theor.		
HoNiGe	5.0	−2.6	11.2	10.61	$5.1\ 10^{-6}$	this work
		−3	10.43			[7]
ErNiGe	2.9	−1.4	9.19	9.58	$5.4\ 10^{-6}$	this work
	6	−4	9.28			[7]

table 2. The values of these parameters are compared with the data in ref. [7].

3.3. Magnetic structure

3.3.1. HoNiGe

The magnetic reflections in the neutron diffraction pattern of HoNiGe obtained at $T = 1.65$ K (see fig. 2) correspond to a magnetic unit cell doubled along the a- and c-axes. The reflections are indexable by h_m, k_m, l_m indices which obey the following rule:

$h_m = h/2, \quad k_m = k, \quad l_m = 1/2;$

h, k, l odd integers.

This indicates a magnetic structure with the propagation vector $k_1 = [1/2, 0, 1/2]$.

The models of magnetic structure were subsequently verified by comparison of calculated and observed intensities. The minimum R factor obtained (see table 3) corresponds to the model in which the magnetic moments located on ions 1 and 2, and also on ions 3 and 4, are coupled ferromagnetically inside the chemical unit cell, but antiferromagnetically between pairs. The Ho atoms form chains running along the a-axis in which the moments are coupled in the sequence $+ + - -$. The magnetic moment is parallel to the a-axis (see fig. 3). The refined value of the magnetic moment of Ho^{3+} ion at $T = 1.65$ K, 9.98(5) μ_B equals the free-ion value for Ho^{3+} ($gJ = 10$).

With an increase in temperature a decrease in intensities corresponding to the collinear structure is observed. New reflections result from a modulated structure. In the neutron patterns at $T = 2.2$ K peaks caused by two types of magnetic structure are observed. The peaks observed in the neutron diffraction pattern obtained at $T = 2.55$ K correspond to a high-temperature phase. These reflections can be indexed with the wavevector $k_1' = [0.469, 0.221, 0.426]$. A three-component

Table 3
Magnetic intensities for HoNiGe: the indices refer to the orthorhombic chemical cell and the reflections $hkl^{\pm}$ are given satellite at $T = 2.55$ K

$T = 1.65$ K					$T = 2.55$ K				
hkl	$2\Theta_{calc}$	$2\Theta_{obs}$	I_{calc}	I_{obs}	hkl	$2\Theta_{calc}$	$2\Theta_{obs}$	I_{calc}	I_{obs}
101	13.98	13.96	1999.9	1998.6	$000^{\pm}$	14.51	14.51	337.9	338.9
103	30.83	30.81	162.2	103.4	101^{-}	17.07	17.06	16.6	21.3
301	32.33	32.22	331.1	322.2	011^{-}	29.44	29.41	67.2	43.3
111	36.50	36.55	109.2	63.0	$10-1^{-}$	30.57	30.58	5.4	5.0
303	41.83	43.88	143.4	72.9	002^{-}	32.84		61.5	
113	46.2	46.23	238.9	255.6	200^{-}	33.35	32.88	62.1	119.0
311	47.27	47.31	144.7	121.5	-101^{-}	33.50		6.0	
105	50.53	50.68	344.7	341.5	$01-1^{-}$	39.34	39.68	49.0	48.3
501	53.54	53.58	114.9	100.7	101^{+}	41.95	41.78	2.3	26.6
313	55.47	55.63	242.0	288.1	211^{-}	42.65		41.6	
305	59.33	59.41	95.3	100.0	$0-11^{-}$	43.7	44.68	48.0	50.6
					202^{-}	45.0		20.5	
					002^{+}	49.44	49.53	51.6	106.0
					$21-1^{-}$	50.16		38.8	
					011^{+}	51.10	51.00	22.3	25.0
					-112^{-}	51.14		5.7	
					103^{-}	52.76		12.4	
					200^{+}	53.08	52.78	24.1	35.0
					$1-12^{-}$	53.18		7.7	
					$2-11^{-}$	53.84	–	19.5	0
					301^{-}	55.03	–	1.4	0
R (%)			7.96					15.4	

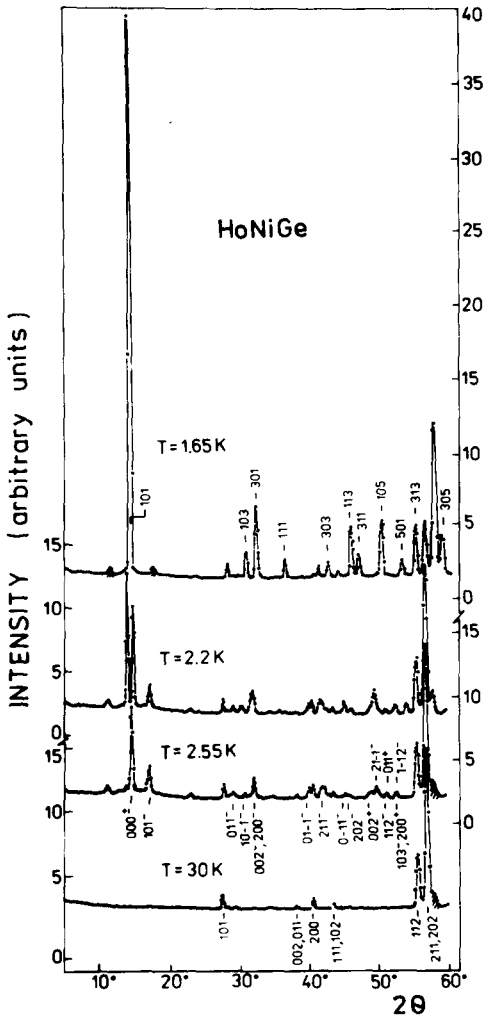

Fig. 2. Neutron diffraction diagram of HoNiGe at various temperatures. The shaded peaks arise from $HoNi_2Ge_2$ impurity.

wavevector describes a modulation in the magnetic structure of either the magnetic moment amplitude (sinusoidal) or of the magnetic moment direction (spiral). On the basis of intensity calculations it has been found that the spiral structure explains the observed intensities better than the sinusoidal one (see table 3). The spiral axis forms an angle of 61(15)° with the c-axis and 16(10)° with the a-axis. The magnetic moment at $T = 2.55$ K is $4.07(10)\mu_B$.

The temperature dependence of the 101 and

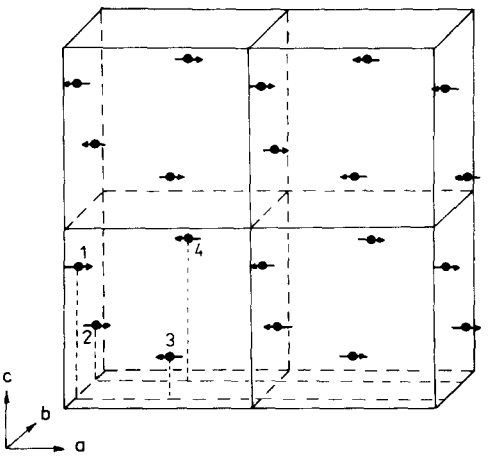

Fig. 3. Magnetic structure of HoNiGe at low temperatures.

$000^{\pm}$ reflections as well as the value of magnetic moment are shown in fig. 4. In the temperature region 2.0–2.5 K the coexistence of two phases is observed. The temperature dependence of the $000^{\pm}$ magnetic reflection indicates the Néel temperature as $T_N = 2.75(5)$ K which is smaller than that given by magnetic measurements (see table 2).

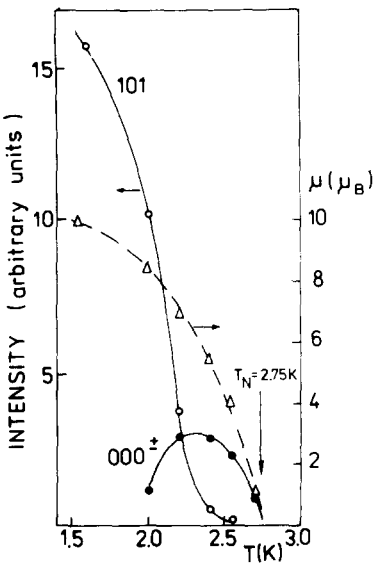

Fig. 4. Temperature dependence of the magnetic intensity of different types of reflection lines associated with two magnetic structures having propagation vectors $k_1 = [1/2, 0, 1/2]$ and $k_1' = [0.469, 0.221, 0.42]$, respectively.

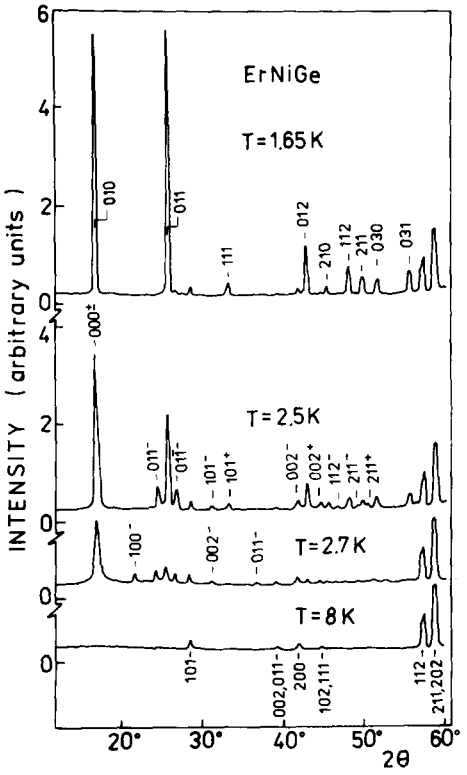

Fig. 5. Neutron diffraction diagram of ErNiGe at various temperatures.

3.3.2. *ErNiGe*

The magnetic reflections observed on the neutron diffraction pattern of ErNiGe recorded at $T = 1.65$ K (see fig. 5) were indexed assuming a magnetic unit cell doubled along the *b*-axis. This corresponds to a magnetic structure with the propagation vector $k_2 = [0, 0.5, 0]$. The models of magnetic structure were verified by comparison of the calculated and observed intensities. The minimum of the *R* factor (see table 4) corresponds to the model in which the magnetic moments are located on the Er^{3+} ions and in which they are coupled $+ - + -$ inside the chemical unit cell, but antiferromagnetically in the magnetic one (see fig. 6a). The magnetic moment is equal to $9.05(5)\mu_B$ and forms an angle of $\psi = 65°$ with the *a*-axis.

With increase in temperature, changes in the diffraction patterns are observed. The diffraction pattern taken at $T = 2.36$ K contains two groups of magnetic reflections. The first group represents the reflections corresponding to the collinear commensurably modulated magnetic structure with the wavevector $k_2 = [0, 0.5, 0]$ observed also at low temperature. The second group of reflections corresponds to the incommensurably modulated component of the magnetic moment. The additional magnetic reflections appear as satellites with the wavevector $k_2' = (0, 0.5, 0.084)$.

The minimum of the reliability factor (see table 4) corresponds to the model for which the magnetic moment parallel to the *b*-axis equals $\mu = 7.04(15)\mu_B$ and forms a sine-modulated structure.

Table 4
Magnetic intensities for ErNiGe: the indices refer to the orthorhombic chemical cell and the reflections $hkl^{\pm}$ are given satellites at $T = 2.5$ K

$T = 1.65$ K					$T = 2.5$ K				
hkl	$2\Theta_{calc}$	$2\Theta_{obs}$	I_{calc}	I_{obs}	*hkl*	$2\Theta_{calc}$	$2\Theta_{obs}$	I_{calc}	I_{obs}
010	16.65	16.63	23.51	2226.4	$000^{\pm}$	16.73	16.80	528.6	532.2
011	25.58	25.58	2032.4	2234.2	011^{-}	24.36	24.40	247.6	244.7
111	33.03	33.03	139.0	110.2	$01-1^{-}$	26.85	26.70	219.4	218.6
012	42.80	42.83	551.8	553.4	101^{-}	32.08	32.10	16.8	13.2
210	45.30	45.33	195.3	67.7	101^{+}	34.05	33.95	15.3	13.2
112	47.93	48.03	297.0	362.6	002^{-}	41.23	41.05	68.9	43.3
211	49.65	49.68	416.3	237.8	002^{+}	44.40	44.60	58.7	54.2
030	51.50	51.63	215.0	202.8	112^{-}	46.5	46.7	35.1	30.0
031	55.5	55.52	344.0	330.6	211^{-}	49.00	49.25	47.7	60.2
R (%)			8.8					5.6	

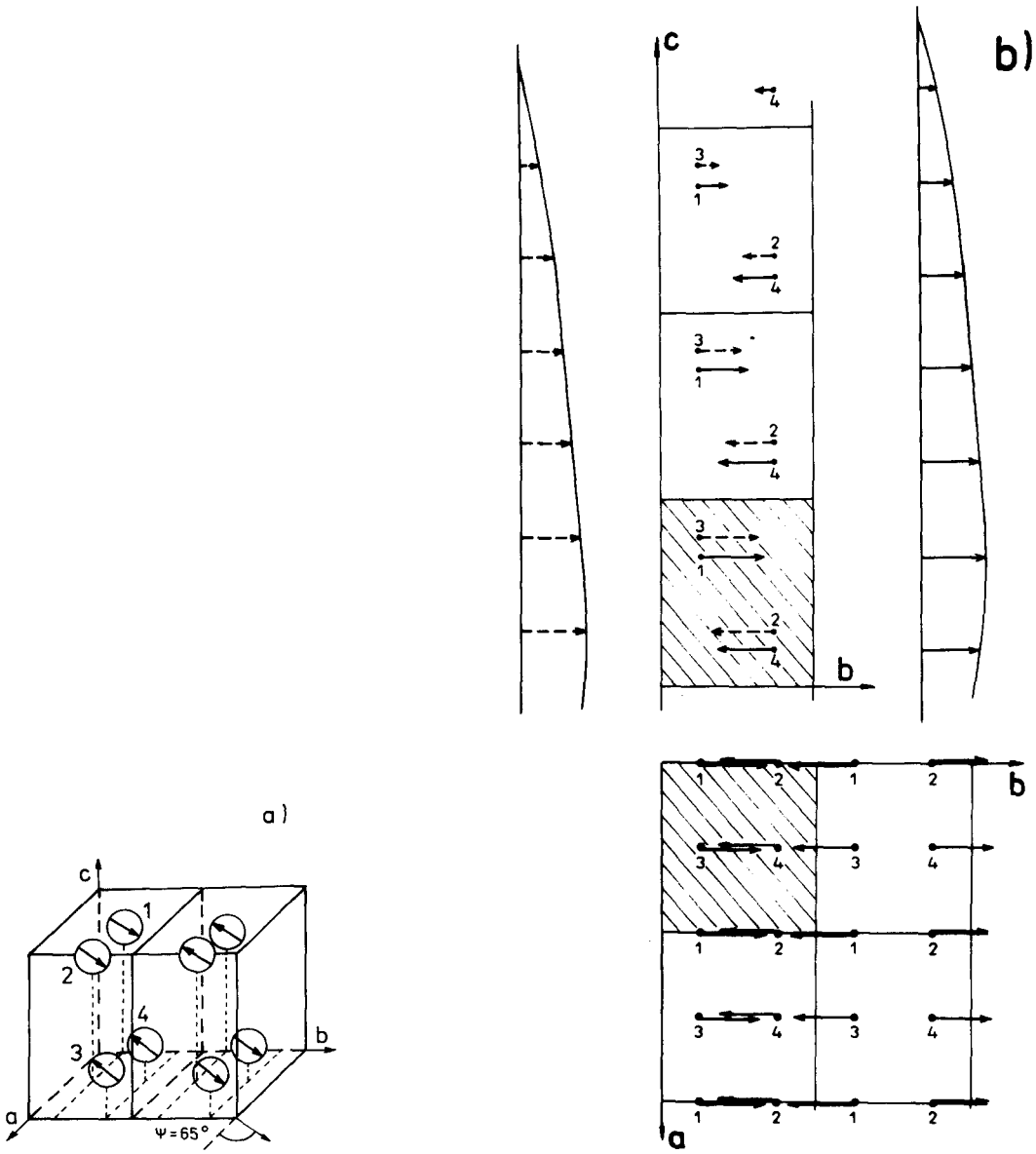

Fig. 6. Magnetic structure of ErNiGe: (a) low-temperature phase, (b) high temperature phase in the projection on the *ab* and *bc* planes.

At $T = 2.7$ K three new reflections are observed. These reflections can be indexed as satellites of the basal reflections with the propagation vector $k = (0, 0, 0.37)$. The analysis of the intensities suggests a modulated magnetic structure. In this pattern peaks corresponding to the previous magnetic structures are observed. This is why a clear description of the magnetic structure of the new phase is difficult.

The temperature dependence of the reflections 010 and 011^- are shown in fig. 7. This dependence indicates the coexistence of two magnetic phases between the temperature 2.36 K and the Néel temperature (2.90(5) K).

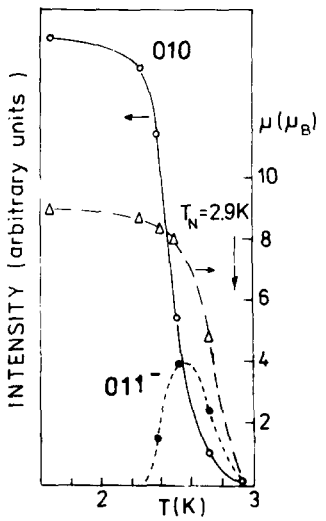

Fig. 7. Temperature dependence of the magnetic reflections 010 and 011^- and value of magnetic moment for ErNiGe.

4. Symmetry analysis

Group-theoretical calculations based on the Bertaut [11] and Izyumov method [12,13] have been made for HoNiGe and ErNiGe.

Group-theoretical calculations known as the symmetry analysis method allow the possibility of finding all models of the magnetic structures admitted by the paramagnetic phase symmetry after the phase transition. These models, regarded as some axial function determined on a given set of equivalent positions with symmetry group G, may be given as the linear combinations of basis vectors of this space group representations:

$$S(\boldsymbol{r}) = \sum_{\nu,\lambda,\lambda} c_\lambda^{\nu l} \psi_\lambda^{\nu l} \qquad (1)$$

(ν, λ and l number the representation, its dimension and arms of $\boldsymbol{k}$ vector, respectively). The so-called 'magnetic representation' may be presented as the direct sum of such number of irreducible representations of the symmetry space group. This representation may appear in (1).

The functions $S(\boldsymbol{r})$ must be real, so when the irreducible representations are complex and the corresponding basis vectors are complex, in the decomposition (1) two conjugate representations have to appear. When the structures are should incommensurate they be described by modes (the parts of basis vectors connected with given positions in the crystal cell) belonging to two arms of the $\boldsymbol{k}$ vector star: $\boldsymbol{k}_1$ and $\boldsymbol{k}_2 = -\boldsymbol{k}_1$.

The linear combination of modes in the form:

$$\begin{aligned} s_n &= M\, e^{ik\cdot t_n} + M^*\, e^{-ik\cdot t_n} \\ &= 2s_0(m_1 + pm_2)\cos(k\cdot t_n), \qquad (2) \\ M &= (m_1 + pm_2); \qquad m_1\cdot m_2 = 0; \qquad m_1^2 = m_2^2 \end{aligned}$$

gives the sine-modulated structure with magnetic moments in the $\boldsymbol{m}_1$, $\boldsymbol{m}_2$ plane. The linear combination in the form:

$$\begin{aligned} S_n &= M\, e^{ik\cdot t_n} + M^*\, e^{-ik\cdot t_n} \\ &= 2s_0(m_1\cdot\cos(k\cdot t_n) + pm_2\cdot\sin(k\cdot t_n)), \\ M &= (m_1 + ipm_2); \qquad m_1\cdot m_2 = 0; \qquad m_1^2 = m_2^2 \qquad (3) \end{aligned}$$

gives the helicoidal ($p = 1$) or elliptic ($p \neq 1$) structure with magnetic moments rotating in the $\boldsymbol{m}_1$, $\boldsymbol{m}_2$ plane. As may be seen from the formulae mentioned above $\boldsymbol{k}$ and $-\boldsymbol{k}$ modes on the same atom position have to be in the same phase.

4.1. HoNiGe

The magnetic representation may be decomposed on eight one-dimensional, complex representations. Some of them appear in this decomposition, twice, some only once. The magnetic structure, presented as the linear combination of the basic functions of these representations must be a real function. Since the star of $\boldsymbol{k}$ vector is only one-armed the magnetic structure must belong to two irreproducible, conjugate representations. The best fit to the experimental results yields the model of the magnetic structure belonging to $\tau_5 \oplus \tau_7$ representations with the order parameter $p = (c\cdot\exp(i\alpha),\ c\cdot\exp(-i\alpha))$. This means that the function $S(\boldsymbol{r}_1)$ describing the magnetic structure may be given as follows:

$$S(\boldsymbol{r}_1) = c\cdot\exp(i\alpha)\cdot\phi_5 + c\cdot\exp(-i\alpha)\cdot\phi_7.$$

The magnetic modes for D_{2h}^{16} symmetry group, 4(c) positions vector $k = [1/2, 0, 1/2]$, τ_5 and τ_7 representations are given in table 5.

Table 5

Repr.	Basis vector	1	2	3	4
τ_5	ϕ_5	(100)	(100)	(i00)	(i00)
τ_5	ϕ_5'	(001)	(001)	(00 −i)	(00 −i)
τ_7	ϕ_7	(100)	(100)	(−i00)	(−i00)
τ_7	ϕ_7'	(001)	(001)	(00i)	(00i)

The corresponding magnetic moments on the 4(c) positions, parallel to the x-axis are:

$$S_{1n} = 2 \cdot c \cdot e_x \cdot \cos(\alpha + k \cdot t_n),$$
$$S_{2n} = 2 \cdot c \cdot e_x \cdot \cos(\alpha + k \cdot t_n),$$
$$S_{3n} = -2 \cdot c \cdot e_x \cdot \sin(\alpha + k \cdot t_n),$$
$$S_{4n} = -2 \cdot c \cdot e_x \cdot \sin(\alpha + k \cdot t_n).$$

For $\alpha = \pi/4$ the magnetic moments on all sites have the same value and translations by primitive lattice vectors along the a- and c-directions change their sign (fig. 3).

4.2. ErNiGe

For $k = [0, 1/2, 0]$ the magnetic representation may be decomposed on two irreducible representations which are both two-dimensional and complex. Each of them appears in this decomposition three times.

The magnetic structure which gives the best fit to the experimental results at $T = 1.65$ K may be presented as the linear combination of basis vectors of representation $\tau = \tau_1 \oplus \tau_1'$ with the order parameter

$$p = (c \cdot \exp(i\pi/2 + i\alpha), c \cdot \exp(i\pi/2 - i\alpha); \\ c' \cdot \exp(i\alpha), c' \cdot \exp(-i\alpha)).$$

This means that the function $S(r)$ describing the magnetic structure may be given as follows:

$$S(r) = c \cdot \exp(i\pi/2 + i\alpha) \cdot \phi_1 + c \cdot \exp(i\pi/2 - i\alpha) \cdot \phi_2 + c' \cdot \exp(i\alpha) \cdot \phi_1' + c' \cdot \exp(-i\alpha) \cdot \phi_2'.$$

The magnetic modes for D_{2h}^{16} symmetry group, 4(c) positions vector $k = [0, 1/2, 0]$ and τ_1 representation are given in table 6.

Table 6

Basis vector	1	2	3	4
ϕ_1	(100)	(−i00)	(100)	(−i00)
ϕ_2	(−100)	(−i00)	(−100)	(−i00)
ϕ_1'	(010)	(0i0)	(010)	(0i0)
ϕ_2'	(010)	(0 −i0)	(010)	(0 −i0)
ϕ_1''	(001)	(00 −i)	(00 −1)	(00i)
ϕ_2''	(00 −1)	(00 −i)	(001)	(00i)

The corresponding magnetic moments on the 4(c) positions parallel to the ab-plane are:

$$S_{1n} = 2 \cdot c \cdot e_x \cdot \sin(\alpha + k \cdot t_n) + 2 \cdot c' \cdot e_y \cdot \cos(\alpha + k \cdot t_n),$$
$$S_{2n} = -2 \cdot c \cdot e_x \cdot \cos(\alpha + k \cdot t_n) - 2 \cdot c' \cdot e_y \cdot \sin(\alpha + k \cdot t_n),$$
$$S_{3n} = 2 \cdot c \cdot e_x \cdot \sin(\alpha + k \cdot t_n) + 2 \cdot c' \cdot e_y \cdot \cos(\alpha + k \cdot t_n),$$
$$S_{4n} = -2 \cdot c \cdot e_x \cdot \cos(\alpha + k \cdot t_n) - 2 \cdot c' \cdot e_y \cdot \sin(\alpha + k \cdot t_n).$$

For $\alpha = \pi/4$ the magnetic moments on all sites have the same value and the translation by primitive lattice vector along the b-direction changes their sign.

For $k_1 = [0, 1/2, 0.084]$ the set of 4(c) position splits on two orbits, which should be calculated independently (atoms 1 and 4 in the one orbit and atoms 2 and 3 in the second).

Table 7

		1	2	3	4
	$^1\phi_1$	100	100	$e^{-i\alpha}$ 00	$e^{i\alpha}$ 00
	$^1\phi_2$	100	−100	$e^{-i\alpha}$	$-e^{i\alpha}$ 00
k_1	$^1\phi_1'$	010	010	0 $e^{-i\alpha}$ 0	0 $e^{i\alpha}$ 0
	$^1\phi_2'$	0 −10	010	0 $-e^{-i\alpha}$ 0	0 $e^{i\alpha}$ 0
	$^1\phi_1''$	001	001	00 $-e^{-i\alpha}$	00 $-e^{i\alpha}$
	$^1\phi_2''$	001	00 −1	00 $-e^{-i\alpha}$	00 $e^{i\alpha}$
	$^2\phi_1$	$e^{-i2\alpha}$ 00	$-e^{-i2\alpha}$ 00	$e^{-i\alpha}$ 00	$-e^{-i3\alpha}$ 00
	$^2\phi_2$	$-e^{-i2\alpha}$ 00	$-e^{-i2\alpha}$ 00	$-e^{-i\alpha}$ 00	$-e^{-i3\alpha}$ 00
k_2	$^2\phi_1'$	0 $-e^{-i2\alpha}$ 0	0 $e^{-i2\alpha}$ 0	0 $-e^{-i\alpha}$ 0	0 $e^{-i3\alpha}$ 0
	$^2\phi_2'$	0 $-e^{-i2\alpha}$ 0	0 $-e^{-i2\alpha}$ 0	0 $-e^{-i\alpha}$ 0	0 $-e^{-i3\alpha}$ 0
	$^2\phi_1''$	00 $e^{-i2\alpha}$	00 $-e^{-i2\alpha}$	00 $-e^{-i\alpha}$	00 $e^{-i3\alpha}$
	$^2\phi_2''$	00 $-e^{-i2\alpha}$	00 $-e^{-i2\alpha}$	00 $e^{-i\alpha}$	00 $e^{-i3\alpha}$

$\alpha = 0.084\pi$.

Table 8

		1	2	3	4
	$^1\phi_1$	100	$e^{i2\alpha}00$	$e^{i\alpha}00$	$e^{i\alpha}00$
	$^1\phi_2$	100	$-e^{i2\alpha}00$	$e^{i\alpha}00$	$-e^{i\alpha}00$
k_1	$^1\phi_1'$	010	$0e^{i2\alpha}0$	$0e^{i\alpha}0$	$0e^{i\alpha}0$
	$^1\phi_2'$	$0-10$	$0e^{i2\alpha}0$	$0-e^{i\alpha}0$	$0e^{i\alpha}0$
	$^1\phi_1''$	001	$00e^{i2\alpha}$	$00-e^{i\alpha}$	$00-e^{i\alpha}$
	$^1\phi_2''$	001	$00e^{i2\alpha}$	$00-e^{i\alpha}$	$00e^{i\alpha}$
	$^2\phi_1$	100	$-e^{-i2\alpha}00$	$e^{-i\alpha}00$	$-e^{-i\alpha}00$
	$^2\phi_2$	-100	$-e^{-i2\alpha}00$	$-e^{-i\alpha}00$	$-e^{-i\alpha}00$
k_2	$^2\phi_1'$	$0-10$	$0e^{-i2\alpha}0$	$0-e^{-i\alpha}0$	$0e^{-i\alpha}0$
	$^2\phi_2'$	$0-10$	$0-e^{-i2\alpha}0$	$0-e^{-i\alpha}0$	$0-e^{-i\alpha}0$
	$^2\phi_1''$	001	$00-e^{-i2\alpha}$	$00-e^{-i\alpha}$	$00e^{-i\alpha}$
	$^2\phi_2''$	$00-1$	$00-e^{-i2\alpha}$	$00e^{-i\alpha}$	$00e^{-i\alpha}$

$\alpha = 0.084\pi$.

In the decomposition of the magnetic representation on to the irreducible ones, the τ_1, two-dimensional complex representation appears three times. The magnetic modes calculated for $\boldsymbol{k}_1$ and $\boldsymbol{k}_2 = -\boldsymbol{k}_1$ are given in table 7.

In order to the magnetic structure as real function, the phase obtain a shift between orbits is required, shown in table 8.

The best fit to the experimental results gives the model of magnetic structure with order parameter $p = (0, c; c, 0)$. So the $S(r_i)$ function may be presented as:

$$S(r_i) = c \cdot {}^1\phi_2' + c \cdot {}^2\phi_1'.$$

The corresponding magnetic moments on the 4(c) positions, parallel to the b direction are:

$$S_{1n} = c \cdot e_y \cdot \cos(k \cdot t_n)$$

$$S_{2n} = -c \cdot e_y \cdot \cos(2\alpha + k \cdot t_n)$$

$$S_{3n} = c \cdot e_y \cdot \cos(\alpha + k \cdot t_n)$$

$$S_{4n} = -c \cdot e_y \cdot \cos(\alpha + k \cdot t_n)$$

where $\alpha = 0.084\ \pi$ (see fig. 6b).

5. Discussion

The ternary RNiGe intermetallic compounds (R = Tb–Er) crystallize in an orthorhombic Ni-TiSi-type crystal structure.

Our previous investigations [14] indicate that TbNiGe and DyNiGe compounds have an orthorhombic TiNiSi-type structure. Both compounds are antiferromagnets with Néel temperatures of 18 and 6 K, respectively. The neutron diffraction data indicate that at low temperatures both compounds have a square-modulated structure with the wavevector $k = (2/3, 1/3, 0)$. With an increase in temperature, a change to a sine-modulated structure for TbNiGe and a change to a cycloidal spiral structure for DyNiGe are observed. In the case of the TbNiGe compound the coexistence of two magnetic over structures a wide temperature range is observed.

The results of this work indicate that at low temperature, the rare earth moments are collinear and with an increase in temperature a change to a sine modulated or a helicoidal structure occurs.

In the RNiGe compounds, rare earth ions form chains running along the a-axis. The R^{3+}–R^{3+} distance in the chain is 3.482 Å. The chains belonging to the adjacent planes are at a R^{3+}–R^{3+} distance of 3.668 Å and form a three-dimensional framework. The magnitudes of the distances indicate that the magnetic interactions are predominantly determined by indirect coupling via conduction electrons or by the super exchange. The oscillatory character of the magnetic ordering at high temperatures implies that the RKKY model of magnetic interactions via conduction electrons can be useful for the description of the magnetic structure. In this model the paramagnetic Curie temperature for heavy rare earth ions is proportional to the de Gennes function [15]. The results presented in ref. [7] show that the paramagnetic Curie temperature Θ_p follows the de Gennes law.

Changes in the magnetic ordering with variation of the temperature could not be using obtained the RKKY model. It was possible, however, to interpret the observed changes in the magnetic structure with temperature on the basis of the ANNNI (anisotropic next-nearest-neighbour Ising) model [16]. In the ANNNI model an interaction between the nearest-neighbour layers is positive ($J_1 > 0$) and an interaction between the next-nearest-neighbour layers is negative ($J_2 < 0$). Mean field calculations produce a collinear magnetic structure at low temperatures and several

non-collinear structures with an increase in temperature.

The values of the Néel temperatures of the RNiGe compound are small. This indicates that the exchange interactions are small, usually of the same magnitude as the crystal-field effects. It may happen that the crystal-field effects induce an important anisotropy. In the orthorhombic unit cell, the four rare earth ions are in the same 4(c) site of a low-symmetry C_2. In such symmetry, the crystal field Hamiltonian can be written as follows:

$$\mathscr{H}_{cf} = \alpha\left(V_2^0 O_2^0 + V_2^2 O_2^2\right) + \beta\left(V_4^0 O_4^0 + V_4^2 O_4^2 + V_4^4 O_4^4\right) + \gamma\left(V_4^0 O_4^0 + V_6^2 O_6^2 + V_6^4 O_6^4 + V_6^6 O_6^6\right),$$

where O_1^m are the equivalent operators, α, β, γ the Stevens factors, and V_1^m are the crystal-field parameters [17].

Nguyen at al. [18] performed point charge calculations for compounds of the RSi series and showed that the magnetic anisotropy is mainly determined by second order crystal field terms. The calculations performed indicate that the moments lie along the a-axis when the parameter is positive (Tb, Dy, Ho), or along the b-axis when $\alpha < 0$ (Er, Tm).

In RNiGe compounds, where R = Tb, Dy and Ho the magnetic moment in both phases is parallel to the a-axis. For ErNiGe at low temperatures the magnetic moment of Er^{3+} ion forms an angle with the a-axis, whereas in the high-temperature phases the magnetic moment is parallel to b-axis.

The deviation of an angle ψ determined by the relation $\mathrm{tg}(\psi) = (V_2^{-2}/V_2^2)$, in ErNiGe at high temperature may result from a strong temperature dependence of the crystal-field parameters.

Acknowledgement

This work has been partially supported by the State Committee for Scientific Research in Poland within Grants 2-0083-91-01 and 2-2438-92-03.

References

[1] E. Hovestreydt, N. Engel, K. Klepp, B. Chabot and E. Parthé, J. Less-Common Metals 85 (1982) 247.
[2] D. Mazzone, R. Rossi, R. Marazza and R. Ferro, J. Less-Common Metals 80 (1981) 47.
[3] P. Rogl, in: Handbook on Physics and Chemistry of Rare Earths, eds. K.A. Gschneidner Jr and L. Eyring (North-Holland, Amsterdam, 1984) vol. 7, p.1.
[4] E. Parthé and B. Chabot, in: Handbook on Physics and Chemistry of Rare Earths, eds. K.A. Gschneidner Jr and L. Eyring (North-Holland, Amsterdam 1984) vol. 7, p.113.
[5] W. Bażela, J. Less-Common Metals 133 (1987) 193.
[6] A. Szytuła, in: Handbook of Magnetic Materials, ed. K.U.J. Buschow (Elsevier, Amsterdam, 1991) vol. 6, p.83.
[7] P.A. Kotsanidis, J.K. Yakinthos and E. Gamari Seale, J. Less-Common Metals 157 (1990).
[8] A. Delapalme, Raport Interne CEA-CNRS/DPh.G. SDN/LLB/85/59.
[9] A.J. Freeman and J.P. Desclaux, J. Magn. Magn. Mater 12 (1979) 11.
[10] H.M. Rietveld, J. Appl. Crystallogr. 2 (1969) 65.
[11] E.F. Bertaut, Acta Crystallogr. A24 (1968) 217.
[12] Yu.A. Izymov and V.E. Naish, J. Magn. Magn. Mater. 12 (1979) 239.
[13] W. Sikora and P. Czopnik, Abstracts of Conference ECM-14, Enschede, 2-7 August 1992, p. 449.
[14] G. André, F. Bourée, M. Kolenda, A. Oleś, A. Pacyna, M. Pinot, W. Sikora and A. Szytuła, J. Magn. Magn. Mater. 116 (1992) 375.
[15] P.G. De Gennes, J. Phys. Radium 23 (1962) S10.
[16] P. Bak and J. von Boehm, Phys. Rev. B21 (1990) 5297.
[17] M.T. Hutchings, in: Solid State Physics, vol. 16, eds. F. Seitz and D. Turnbull (Academic Press, New York, 1964) p. 227.
[18] V.N. Nguyen, J. Rossat-Mignod and F. Tchéou, Solid State Commun. 17 (1975) 101.